Detailed balance analysis of nanophotonic solar cells

Sunil Sandhu, Zongfu Yu, and Shanhui Fan*

Department of Electrical Engineering, Stanford University, Stanford, California 94305, USA

*shanhui@stanford.edu

Abstract: We present a detailed balance based approach for performing current density-voltage characteristic modeling of nanophotonic solar cells. This approach takes into account the intrinsic material non-idealities, and is useful for determining the theoretical limit of solar cell efficiency for a given structure. Our approach only requires the cell's absorption spectra over all angles, which can be readily calculated using available simulation tools. Using this approach, we elucidate the physics of open-circuit voltage enhancement over bulk cells in nanoscale thin film structures, by showing that the enhancement is related to the absorption *suppression* in the immediate spectral region above the bandgap. We also show that with proper design, the use of a grating on a nanoscale thin film can increase its short-circuit current, while preserving its voltage-enhancing capabilities.

OCIS codes: (350.6050) Solar Energy; (350.4238) Nanophotonics and photonic crystal; (310.6628) Subwavelength structures, nanostructures; (050.0050) Diffraction and gratings.

References and links

1. D. Redfield, "Unified model of fundamental limitations on the performance of silicon solar cells," IEEE Trans. Electron. Dev. **27**, 766–771 (1980).
2. T. Tiedje, E. Yablonovitch, G. D. Cody, and B. G. Brooks, "Limiting efficiency of silicon solar cells," IEEE Trans. Electron. Dev. **31**, 711–716 (1984).
3. O. D. Miller, E. Yablonovitch, and S. R. Kurtz, "Strong internal and external luminescence as solar cells approach the shockley-queisser limit," IEEE J. Photovolt. **2**, 303–311 (2012).
4. H. A. Atwater, "Paths to high efficiency low-cost photovoltaics," in "Photovoltaic Specialists Conference (PVSC), 2011 37th IEEE," (2011), pp. 000001–000003.
5. A. Shah, P. Torres, R. Tscharner, N. Wyrsch, and H. Keppner, "Photovoltaic technology: The case for thin-film solar cells," Science **285**, 692–698 (1999).
6. S. Pillai, K. R. Catchpole, T. Trupke, and M. A. Green, "Surface plasmon enhanced silicon solar cells," J. Appl. Phys. **101**, 093105 (2007).
7. L. Hu and G. Chen, "Analysis of optical absorption in silicon nanowire arrays for photovoltaic applications," Nano Lett. **7**, 3249–3252 (2007).
8. A. Chutinan and S. John, "Light trapping and absorption optimization in certain thin-film photonic crystal architectures," Phys. Rev. A **78**, 023825 (2008).
9. L. Zeng, P. Bermel, Y. Yi, B. A. Alamariu, K. A. Broderick, J. Liu, C. Hong, X. Duan, J. Joannopoulos, and L. C. Kimerling, "Demonstration of enhanced absorption in thin film si solar cells with textured photonic crystal back reflector," Appl. Phys. Lett. **93**, 221105 (2008).
10. C. Lin and M. L. Povinelli, "Optical absorption enhancement in silicon nanowire arrays with a large lattice constant for photovoltaic applications," Opt. Express **17**, 19371–19381 (2009).
11. P. N. Saeta, V. E. Ferry, D. Pacifici, J. N. Munday, and H. A. Atwater, "How much can guided modes enhance absorption in thin solar cells?" Opt. Express **17**, 20975–20990 (2009).
12. R. A. Pala, J. White, E. Barnard, J. Liu, and M. L. Brongersma, "Design of plasmonic thin-film solar cells with broadband absorption enhancements," Adv. Mater. **21**, 3504–3509 (2009).
13. S. B. Mallick, M. Agrawal, and P. Peumans, "Optimal light trapping in ultra-thin photonic crystal crystalline silicon solar cells," Opt. Express **18**, 5691–5706 (2010).

#181089 - $15.00 USD Received 4 Dec 2012; revised 23 Dec 2012; accepted 1 Jan 2013; published 10 Jan 2013

14. X. Sheng, S. G. Johnson, J. Michel, and L. C. Kimerling, "Optimization-based design of surface textures for thin-film si solar cells," Opt. Express **19**, A841–A850 (2011).
15. A. Raman, Z. Yu, and S. Fan, "Dielectric nanostructures for broadband light trapping in organic solar cells," Opt. Express **19**, 19015–19026 (2011).
16. E. R. Martins, J. Li, Y. Liu, J. Zhou, and T. F. Krauss, "Engineering gratings for light trapping in photovoltaics: The supercell concept," Phys. Rev. B **86**, 041404 (2012).
17. C. O. McPheeters and E. T. Yu, "Computational analysis of thin film ingaas/gaas quantum well solar cells with back side light trapping structures," Opt. Express **20**, A864–A878 (2012).
18. M. G. Deceglie, V. E. Ferry, A. P. Alivisatos, and H. A. Atwater, "Design of nanostructured solar cells using coupled optical and electrical modeling," Nano Lett. **12**, 2894–2900 (2012).
19. N. Huang, C. Lin, and M. L. Povinelli, "Limiting efficiencies of tandem solar cells consisting of iii-v nanowire arrays on silicon," J. Appl. Phys. **112**, 064321 (2012).
20. A. Niv, M. Gharghi, C. Gladden, O. D. Miller, and X. Zhang, "Near-field electromagnetic theory for thin solar cells," Phys. Rev. Lett. **109**, 138701 (2012).
21. Z. Yu, A. Raman, and S. Fan, "Fundamental limit of nanophotonic light trapping in solar cells," Proc. Natl. Acad. Sci. U.S.A. **107**, 17491–17496 (2010).
22. S. M. Rytov, Y. A. Kravtsov, and V. I. Tatarskii, *Principles of Statistical Radiophysics 3*, 1st ed. (Springer-Verlag, New York, 1989), chap. 3.
23. C. Luo, A. Narayanaswamy, G. Chen, and J. D. Joannopoulos, "Thermal radiation from photonic crystals: A direct calculation," Phys. Rev. Lett. **93**, 213905 (2004).
24. W. Shockley and H. J. Queisser, "Detailed balance limit of efficiency of p-n junction solar cells," J. Appl. Phys. **32**, 510–519 (1961).
25. National Renewable Energy Lab (NREL), http://rredc.nrel.gov/solar/spectra/am1.5/, *Air Mass 1.5 (AM1.5) Global Spectrum (ASTM173-03G)* (2008).
26. L. D. Landau and E. M. Lifshitz, *Statistical Physics Part 1*, 3rd ed. (Elsevier Butterworth-Heinemann, Waltham, MA, 1980), chap. V, pp. 183–190.
27. V. Liu and S. Fan, "S4 : A free electromagnetic solver for layered periodic structures," Comput. Phys. Commun. **183**, 2233–2244 (2012).
28. E. D. Palik, *Handbook of Optical Constants of Solids: Volume 1* (Elsevier Academic Press, Waltham, MA, 1985), pp. 429–443.
29. D. Hill and P. T. Landsberg, "A formalism for the indirect auger effect. i," Proc. R. Soc. Lond. A Math. Phys. Sci. **347**, 547–564 (1976).
30. W. Shockley and W. T. Read, "Statistics of the recombinations of holes and electrons," Phys. Rev. **87**, 835–842 (1952).
31. R. N. Hall, "Electron-hole recombination in germanium," Phys. Rev. **87**, 387–387 (1952).
32. S. M. Sze and M.-K. Lee, *Semiconductor Devices: Physics and Technology*, 3rd ed. (Wiley, New York, NY, 2012), chap. 2, pp. 60–62.
33. C.-C. Chang, C.-Y. Chi, M. Yao, N. Huang, C.-C. Chen, J. Theiss, A. W. Bushmaker, S. LaLumondiere, T.-W. Yeh, M. L. Povinelli, C. Zhou, P. D. Dapkus, and S. B. Cronin, "Electrical and optical characterization of surface passivation in gaas nanowires," Nano Lett. **12**, 4484–4489 (2012).
34. G. Mariani, A. Scofield, and D. Huffaker, "High-perfomance patterned arrays of core-shell gaas nanopillar solar cells with in-situ ingap passivation layer," in "Photovoltaic Specialists Conference (PVSC), 2012 38th IEEE," (2012), pp. 003080–003082.
35. N. Tajik, Z. Peng, P. Kuyanov, and R. R. LaPierre, "Sulfur passivation and contact methods for gaas nanowire solar cells," Nanotechnology **22**, 225402 (2011).
36. U. Strauss, W. W. Ruhle, and K. Kohler, "Auger recombination in intrinsic gaas," Appl. Phys. Lett. **62**, 55–57 (1993).
37. M. Green, "Limits on the open-circuit voltage and efficiency of silicon solar cells imposed by intrinsic auger processes," IEEE Trans. Electron. Dev. **31**, 671–678 (1984).
38. R. F. Pierret, *Semiconductor Fundamentals: Volume 1*, 2nd ed. (Prentice Hall, Upper Saddle River, NJ, 1988), chap. 2, pp. 27,31.
39. B. Kayes, H. Nie, R. Twist, S. Spruytte, F. Reinhardt, I. Kizilyalli, and G. Higashi, "27.6% conversion efficiency, a new record for single-junction solar cells under 1 sun illumination," in "Photovoltaic Specialists Conference (PVSC), 2011 37th IEEE," (2011), pp. 000004–000008.

1. Introduction

The performance of any solar cell is characterized by its current density-voltage (J-V) relationship. Therefore, it is useful to calculate this J-V relation theoretically. For bulk structures, to calculate the J-V relations, there have been two complimentary approaches. In the first approach [1], one performs a combined electrical and optical modeling of a particular device

#181089 - $15.00 USD Received 4 Dec 2012; revised 23 Dec 2012; accepted 1 Jan 2013; published 10 Jan 2013

structure, including the detailed carrier dynamics of the device. In the second approach [2, 3], one instead calculates the limiting efficiency based on the principle of detailed balance and taking into account only the intrinsic material non-idealities. Both these approaches are important. The first approach is crucial in understanding the detailed performance of a particular device, whereas the second approach provides a fundamental limit in terms of efficiency for a given class of structures or materials.

In recent years there have been strong interests in the study of nanophotonic solar cells as a way to improve solar cell efficiency and reduce cost [4, 5]. Most of the simulations of these nanophotonic cells have been focussed on calculating the absorption properties of the device in order to determine the short-circuit current enhancement [6–17]. There has also been work towards combining the optical and electrical simulations of these devices [18, 19]. Complimentary to these works, it is of interest to pursue calculations based on the principle of detailed balance in order to determine the limiting efficiency of a given structure. Reference [20] performed one such study on a GaAs thin film cell with nanoscale film thickness, and showed that the open-circuit voltage in such a thin film can be significantly enhanced beyond that of bulk cells. This obviously has important implications in improving solar cell efficiency, and in reducing material usage and solar cell cost. However, Ref. [20] only considered a flat film and, consequently, the absorption and short-circuit current of their structure suffers significantly as compared to bulk cells. A natural approach to enhance the short-circuit current would be to introduce light trapping in these nanophotonic structures [21]. An important open question, therefore, is whether the physics of voltage enhancement can be preserved in a nanoscale thin film after light trapping is introduced.

To address this question, one will need to do a detailed balance analysis of nanophotonic solar cells. In Ref. [20], this analysis was performed by a direct calculation of the thermal emission of thin film cells using the fluctuation-dissipation theorem [22]. It is well known that such a direct calculation is quite involved for nanophotonic structures [23].

In this paper we introduce an alternative approach for the detailed balance analysis of a nanophotonic solar cell. We show that the absorption spectrum of a solar cell at all angles, as one routinely calculates in solar cell optical modeling, is in fact sufficient for determining the limiting open-circuit voltage, leading to a far easier way to perform solar cell J-V characteristics modeling as compared to the direct emission calculation in Ref. [20]. Our approach, moreover, can be readily generalized to include intrinsic material non-idealities. Using our approach, we numerically demonstrate that a grating structure on a nanoscale thin film can indeed enhance the short-circuit current while preserving the open-circuit voltage enhancement of the thin film, as shown in Fig. 1. We also elucidate the underlying physics of open-circuit voltage enhancement by showing that it is related to the *suppression* of absorption and, hence, thermal emission, in the frequency range immediately above the bandgap.

2. Computational procedure

We first outline the procedure that we use to calculate the J-V characteristics. We start with the detailed balance equation in Ref. [24], which is applicable to solar cells in general:

$$F_{\mathrm{s}} - F_{\mathrm{c}}(V) + R(0) - R(V) - J/q = 0. \tag{1}$$

In Eq. (1), V is the voltage across the cell, J is the current density generated by the cell, and q is the electron charge. F_s is the radiative generation rate per unit area of hole-electron pairs by the incident sunlight, while $F_{\mathrm{c}}(V)$ is the corresponding radiative recombination rate per unit area. $R(0)$ and $R(V)$ are the rates of non-radiative recombination and generation, respectively, of hole-electron pairs per unit area [24]. These non-radiative rates are equal at the thermal equilibrium condition $V = 0$.

#181089 - $15.00 USD Received 4 Dec 2012; revised 23 Dec 2012; accepted 1 Jan 2013; published 10 Jan 2013

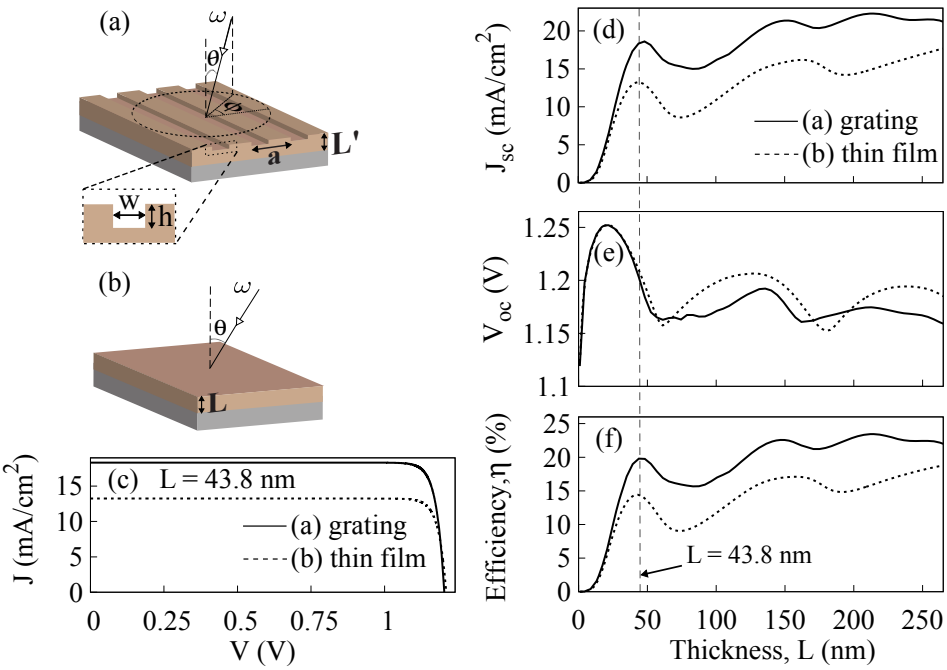

Fig. 1. (a) GaAs grating nanostructure (gold color) with effective thickness $L = \left(1 - \frac{wh}{L'a}\right)L'$ where L' is its actual thickness, a is its periodicity, and each air groove has width w and depth h, (b) GaAs thin film (gold color) with thickness L. Both structures in (a) and (b) have a perfect reflecting back surface (grey color). Also shown in (a) and (b) is the propagation direction of an incident plane wave with frequency ω, polar angle θ, and azimuthal angle ϕ [ϕ is omitted for the azimuthally symmetric thin film in (b)]. (c) shows the J-V curves for the structures in (a) and (b) with thickness L = 43.8 nm. (d)-(f) shows the following characteristics versus thickness L for the structures in (a) and (b): (d) short-circuit current density J_{sc}, (e) open-circuit voltage V_{oc}, and (f) efficiency η. In (c)-(f), the grating structure has periodicity a = 456 nm, and air-groove dimensions ($w = 0.24\,a, h = 0.52\,L'$).

We consider the scenario where the solar cell is under direct sunlight with an incident solar photon rate $S(\omega)$ per unit bandwidth per unit area at a frequency ω. For all our calculations, we used the AM 1.5 global spectrum standard [25] for $S(\omega)$. We also assume the cell has an absorption spectra of $A(\omega,\theta,\phi)$ where θ and ϕ are the incident polar and azimuthal angles, respectively [Fig. 1(a)]. $A(\omega,\theta,\phi)$ here is the sum of the absorbing spectras for both the transverse electric and transverse magnetic incident polarizations. The radiative generation rate F_s in Eq. (1) can be calculated as follows [24]:

$$F_{\mathrm{s}} = \int_{\omega_{\mathrm{g}}}^{\infty} d\omega\, S(\omega) A(\omega, \theta = 0, \phi = 0) \tag{2}$$

where the integration is taken over all frequencies ω starting from the cell's material bandgap frequency ω_{g}.

The radiative recombination rate $F_c(V)$ in Eq. (1) relates to the voltage V across the cell as follows [24]:

$$F_{\mathrm{c}}(V) = F_{\mathrm{co}} \exp\left(\frac{qV}{kT_{\mathrm{c}}}\right) \tag{3}$$

#181089 - $15.00 USD Received 4 Dec 2012; revised 23 Dec 2012; accepted 1 Jan 2013; published 10 Jan 2013

where F_{co} is the radiative recombination rate when the cell is in thermal equilibrium with a surrounding blackbody, k is the Boltzman constant, and T_c is the temperature of the cell. Assuming that our cell has a perfectly reflecting back surface as in the case of the nanostructures in Figs. 1(a)-1(b), F_{co} is then just the thermal emission through the 2π solid angle of the front surface of the cell [26]:

$$F_{co} = \int_0^{2\pi} d\phi \int_0^{\frac{\pi}{2}} d\theta \int_{\omega_g}^{\infty} d\omega \, \Theta(\omega) \, A(\omega,\theta,\phi) \cos(\theta) \sin(\theta). \tag{4}$$

where $\Theta(\omega) = \frac{\omega^2}{4c^2\pi^3}\left[\exp\left(\frac{\hbar\omega}{kT_c}\right) - 1\right]^{-1}$ is *Planck's law* [26] for the incident spectral photon flux density from a surrounding blackbody at a temperature T_c, c is the speed of light in vacuum, and $\hbar$ is the reduced Planck constant. In Eq. (4), we have used *Kirchoff's law* [26] to relate the thermal emission rate of the cell to its absorption spectra $A(\omega,\theta,\phi)$.

The short-circuit current J_{sc} of the cell can be obtained by setting $V = 0$ in Eq. (1) [24]:

$$J_{sc} = q(F_s - F_{co}). \tag{5}$$

And by setting $J = 0$ in Eq. (1) we get the following equation from which we can solve for the open-circuit voltage V_{oc} across the cell [24]:

$$F_s + R(0) = F_c(V_{oc}) + R(V_{oc}). \tag{6}$$

In the case of solar cells where the contribution from non-radiative processes is small as compared to radiative processes, the cell's V_{oc} in Eq. (6) can be approximated as follows:

$$V_{oc} \approx \frac{kT_c}{q} \log\left(\frac{F_s}{F_{co}}\right). \tag{7}$$

From Eqs. (1)-(7), we see that having the absorption spectra $A(\omega,\theta,\phi)$ over all angles is sufficient for the detailed balance analysis of nanophotonic solar cells. Such spectra controls both the absorption and the emission properties of the cell that enters into *Shockley-Queisser's analysis* [24].

The absorption spectra $A(\omega,\theta,\phi)$ can be readily calculated using available simulation tools such as the Rigorous Coupled Wave Analysis (RCWA) [27]. RCWA is a frequency-domain computation tool that can perform a full electromagnetic analysis of layered structures. All absorption spectras $A(\omega,\theta,\phi)$ for the cells discussed in this paper were calculated using the freely available RCWA package in Ref. [27]. The only material related quantity required by these calculations is the solar cell's complex permittivity as a function of frequency. For the GaAs cells discussed in the following sections, this permittivity data was obtained from Ref. [28].

3. Results on a GaAs thin film with and without the grating

In the following, we will first present the results of the J-V characteristics associated with the calculated absorption spectra for the nanostructures shown in Figs. 1(a)-1(b). We specialize to a GaAs cell with a perfect back reflector. For such a cell, the important non-radiative recombination mechanisms in Eq. (1) are Auger recombination, the defect mediated Shockley-Read-Hall effect, and surface recombination [19, 29–35]. Furthermore, since we want to establish an upper bound in the solar cell's performance, we idealize to the case of a defect free GaAs cell with perfect surface passivation. Under these conditions, the only important non-radiative mechanism in our detailed balance analysis is Auger recombination which is given by [36, 37]:

$$R(V) = C_n L n^2 p + C_p L p^2 n \tag{8}$$

#181089 - $15.00 USD Received 4 Dec 2012; revised 23 Dec 2012; accepted 1 Jan 2013; published 10 Jan 2013

where n (p) is the electron (hole) concentration, $C_{\rm n}$ $\left(C_{\rm p}\right)$ is the conduction-band (valance-band) Auger coefficient, and L is the thickness of the cell. In addition, we also assume that the GaAs cell is approximately intrinsic under illumination (i.e. $n \approx p$). In this intrinsic approximation, the Auger recombination rate [Eq. (8)] is minimized and given by [2, 3]:

$$R(V) = \left(C_{\rm n} + C_{\rm p}\right) L\, n_{\rm i}^3 \exp\left(\frac{3qV}{2kT_{\rm c}}\right) \tag{9}$$

where $n_{\rm i}$ is the intrinsic carrier concentration. In all our calculations, we consider GaAs cells operating at a temperature of $T_{\rm c}$ = 300K, where $C_{\rm n} + C_{\rm p} = 7 \times 10^{-30}{\rm cm}^6 \cdot {\rm s}^{-1}$ [36] and $n_{\rm i} = 2 \times 10^6 {\rm cm}^{-3}$ [38].

Although we do include Auger recombination [Eq. (9)] in all our calculations below, we note that for the GaAs solar cells we consider in this paper, this non-radiative rate is small when compared to the radiative rate. Therefore, Eq. (7), which ignores non-radiative recombination, is relevant for these solar cells. The validity of this approximation [Eq. (7)] has also been experimentally verified for micron thick GaAs solar cells in Ref. [39]. We emphasize that one cannot, in general, ignore non-radiative recombination for most solar cell materials. Hence, one should not use Eq. (7) in general. For example, in the case of Si solar cells, the contribution from Auger recombination in Eq. (6) is significant when compared to the radiative recombination rate [2].

The dashed line in Fig. 1(c) plots the J-V curve of a flat GaAs thin film structure [Fig. 1(b)] with thickness L = 43.8 nm. The use of the thin film results in a $V_{\rm oc}$ of 1.21V, which is significantly higher than the $V_{\rm oc}$ of 1.12V for bulk GaAs cells [20]. This result indicates a very important potential of nanoscale thin film structures for enhancing solar cell performance. However, the $J_{\rm sc}$ of the thin film suffers significantly as compared to that of GaAs bulk cells [3]. One natural way to enhance the $J_{\rm sc}$ of the thin film is by introducing light trapping [21]. We therefore consider the grating structure shown in Fig. 1(a). The solid line in Fig. 1(c) shows the J-V curve associated with an optimized grating structure with an effective thickness of $L = \left(1 - \frac{wh}{L'a}\right) L' = 43.8$ nm where $L' = 50$ nm is the actual grating structure thickness, $a = 456$ nm is the grating periodicity, and ($w = 0.24\, a, h = 0.52\, L'$) are the (width, height) of the grating's air groove [Fig. 1(a)]. [The definiton of the effective thickness here is such that different structures with the same effective thickness have the same amount of absorbing material.] Figure 1(c) shows a large enhancement in the $J_{\rm sc}$ of the grating structure relative to that of the thin film. Moreover, the $V_{\rm oc}$ of the grating structure is maintained at approximately the same enhanced value as that of the thin film.

Figures 1(d)-1(f) compares the $J_{\rm sc}$, $V_{\rm oc}$ and efficiency (η) of the thin film and the grating structure for a wide range of thicknesses L. The efficiency here is defined as $\eta = {\rm FF}\frac{J_{\rm sc} V_{\rm oc}}{P_{\rm inc}} \times 100\%$ where $P_{\rm inc}$ is the total incident sun radiation power per unit cell area, and FF is the cell's fill-factor [24]. The grating structures in Figs. 1(d)-1(f) have a periodicity a = 456 nm, and air groove dimensions ($w = 0.24\, a, h = 0.52\, L'$) [Fig. 1(a)]. We see that, in general, the grating structures maintain the same $V_{\rm oc}$ enhancement as in the thin films while still drastically improving the $J_{\rm sc}$ and, hence, the efficiency of such thin solar cell structures.

4. Physics of voltage enhancement

To illustrate the physics of $V_{\rm oc}$ enhancement in nanophotonic structures, we first examine the thermal emission properties of an $L = 10$ μm thick bulk structure with multi-layer anti-reflection coating on its front surface. Figure 2(a) shows its absorptivity spectra as a function of incident polar angle θ. We see that the absorptivity of the bulk structure is ~ 100% for almost all polar angles and wavelengths up to the GaAs band edge at ~ 870 nm [38]. This strong absorptivity results in a strong radiative generation rate $F_{\rm s}$ [Eq. (2)] and, consequently, a $J_{\rm sc}$ of 31.6mA,

#181089 - $15.00 USD Received 4 Dec 2012; revised 23 Dec 2012; accepted 1 Jan 2013; published 10 Jan 2013

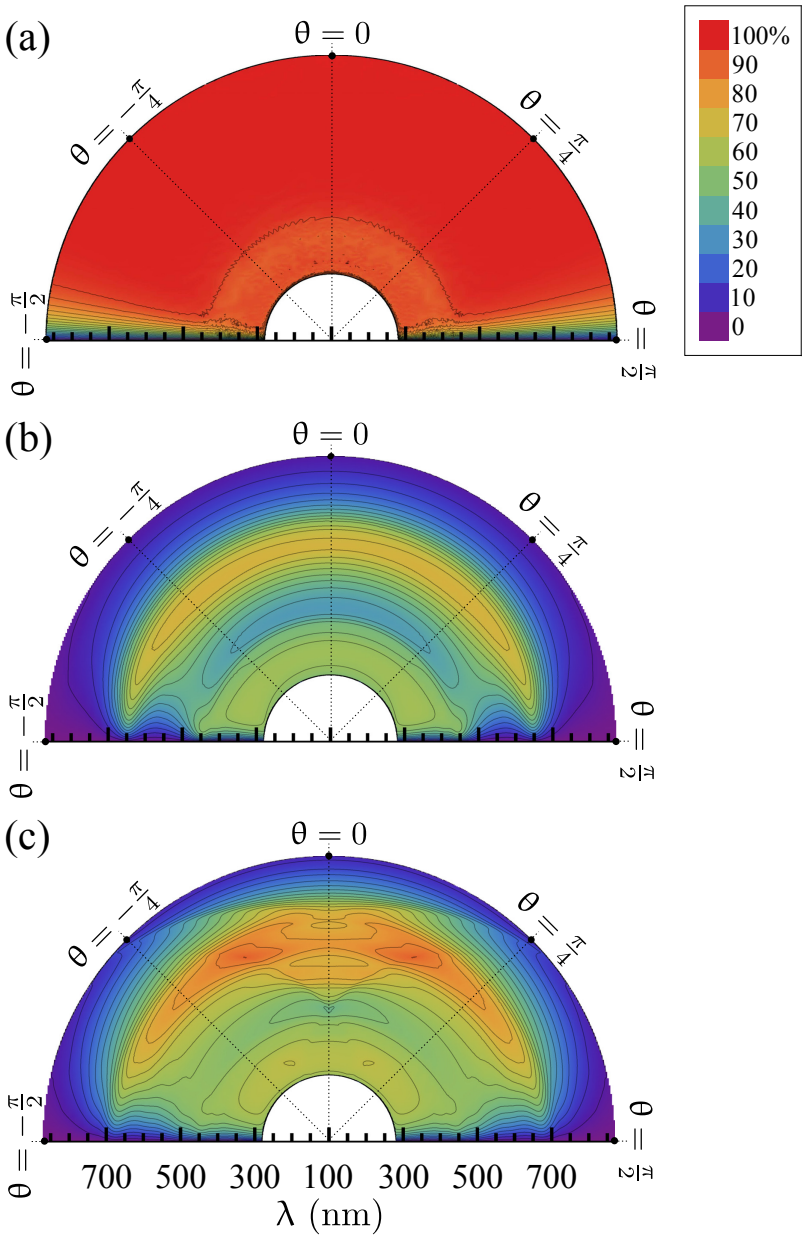

Fig. 2. Contour-density plots of absorptivity spectra for different polar angles θ of: (a) an $L = 10$ μm thick bulk GaAs structure with a multi-layer anti-reflection coating on its front surface, (b) thin film structure associated with dashed J-V curve in Fig. 1(c), and (c) grating structure associated with solid J-V curve in Fig. 1(c). The plot in (c) includes an integration over all azimuthal angles ϕ for each polar angle θ. The absorptivity in all plots is the mean absorptivity of the transverse electric and transverse magnetic incident polarizations.

#181089 - $15.00 USD Received 4 Dec 2012; revised 23 Dec 2012; accepted 1 Jan 2013; published 10 Jan 2013

which is close to the maximum possible J_{sc} for a GaAs solar cell [3]. However, this strong absorptivity also results in a thermal equilibrium recombination rate F_{co} [Eq. (4)] that is close to the maximum value for GaAs. Therefore, the contrast between F_s and F_{co} is low [Eq. (7)], resulting in a V_{oc} of 1.16V, which is significantly lower than the enhanced V_{oc} of the nanostructures associated with the J-V curves in Fig. 1(c).

Figure 2(b) shows the absorptivity spectra for the thin film associated with the dashed J-V curve in Fig. 1(c). The key difference from the bulk structure's spectra in Fig. 2(a) is the thin film's strong absorption suppression in the region of the GaAs band edge at ~ 870 nm for all polar angles θ. Such absorption suppression in the immediate frequency range above the bandgap in Fig. 2(b) results in a large reduction of the thin film's thermal equilibrium recombination rate F_{co}. This can be seen by examining the spectral integration above the bandgap frequency ω_g in Eq. (4). Since the cell is operating at a temperature T_c that satisfies $kT_c \ll \hbar\omega_g$, the thermal emission photon flux spectrum $\Theta(\omega)$ in Eq. (4) can be approximated as:

$$\Theta(\omega) \approx \frac{\omega^2}{4c^2\pi^3} \exp\left(-\frac{\hbar\omega}{kT_c}\right) H(\omega - \omega_g) \tag{10}$$

where $H(\cdot)$ is the Heaviside step function. Therefore, the thermal emission spectrum of the cell is located immediately above the bandgap and has a relatively narrow width of kT_c. Accordingly, reducing the absorption of the cell in this frequency range will have a very strong influence on the cell's thermal emission and, hence, strongly influences F_{co}. On the other hand, the thermal emission spectral width corresponds only to a very small fraction of the total absorption bandwidth of the cell. Moreover, since the solar radiation has a much wider bandwidth, reducing the absorption in the immediate frequency range above the bandgap has far less influence on the radiative generation rate F_s. Therefore, it follows that reducing the absorption in the immediate frequency range above the bandgap increases the contrast between F_s and F_{co} [Eq. (7)] and, consequently, leads to the enhancement of the structure's V_{oc}.

For the thin film's absorptivity spectra in Fig. 2(b), we see that there is also a strong reduction of absorption at normal incidence $\theta = 0$ over the entire frequency range above the bandgap as compared to the bulk structure's spectra in Fig. 2(a). This leads to a significant reduction of the J_{sc} in the thin film case. However, as illustrated above, the V_{oc} and J_{sc} are really controlled by different parts of the absorptivity spectra. This observation motivates incorporating light trapping [21] into the thin film so as to possibly: (i) enhance the solar radiation absorption away from the bandgap region in order to enhance the thin film's J_{sc}, and (ii) still preserve the absorption suppression in the kT_c region immediately above the bandgap in order to maintain the V_{oc} enhancement over the bulk structure. The optimized grating structure associated with the solid J-V curve in Fig. 1(c) indeed has such characteristics in its absorptivity spectra [Fig. 2(c)]. In particular, the spectra in Fig. 2(c) preserves the absorption suppression in the spectral region immediately above the GaAs bandgap. Consequently, the grating structure has a V_{oc} of 1.2V, which is a large enhancement over the bulk structure, and similar to the V_{oc} of the thin film with equivalent thickness L [Fig. 1(c)]. In addition, the grating's enhanced absorption, away from the GaAs bandgap region, at the normal incidence angle $\theta = 0$ [Fig. 2(c)] results in a large J_{sc} enhancement over the thin film as shown in Fig. 1(c).

5. Conclusion

In summary, we presented a computational tool for the detailed balance analysis of solar cell efficiency, and elucidated the physics of open-circuit voltage enhancement by analyzing the angular and spectral distribution of the cell's absorption spectrum. We showed that the open-circuit voltage (V_{oc}) and the short-circuit current (J_{sc}) are controlled by different parts of the cell's absorption spectrum, and that the V_{oc} can be enhanced by suppressing the absorption in

#181089 - $15.00 USD Received 4 Dec 2012; revised 23 Dec 2012; accepted 1 Jan 2013; published 10 Jan 2013

the immediate vicinity of the material's bandgap. Our analysis here, moreover, indicates other opportunities for creating a cell with high V_{oc} and J_{sc}. For example, in the angular integral within Eq. (4), the cell's absorption strength is modulated by a $\sin(2\theta)$ factor. Therefore, the absorption strength in the immediate vicinity of $\theta = 0$ and $\theta = \frac{\pi}{2}$ has a negligible contribution to the thermal equilibrium recombination rate F_{co}. However, strengthening the absorption at the normal incidence angle $\theta = 0$ does enhance the cell's radiative generation rate F_s [Eq. (2)]. These observations together with Eq. (5) and Eq. (7) indicate that: (i) significant V_{oc} enhancement due to absorption suppression comes only from the angular region away from $\theta = 0$ and $\theta = \frac{\pi}{2}$ with spectral width kT_c immediately above the bangap, and (ii) strengthening the absorption at $\theta = 0$ leads to both V_{oc} and J_{sc} enhancement. We anticipate that our analysis tool will prove useful to understand the ultimate performance of nanophotonic solar cells in general.

Acknowledgments

This work is supported by the Department of Energy Grant No. DE-FG07ER46426, by the Department of Energy Bay Area Photovoltaics Consortium (BAPVC), and by the Global Climate and Energy Project (GCEP) of Stanford University. The simulations were performed at the Trestles cluster of the San Diego Supercomputer Center supported by an NSF XSEDE allocation.

#181089 - $15.00 USD Received 4 Dec 2012; revised 23 Dec 2012; accepted 1 Jan 2013; published 10 Jan 2013